Brain magnetic resonance imaging findings in hyperammonemic hepatic encephalopathy: A case series and literature review

AHMED BAKHARJI[1], HUSSAIN ALARFAJ[2], SAMEEH OMAR[1], SULTAN ALZAHRANI[1], NAIF ALZAHRANI[1], FAWZIYA ALAHMARI[1], SIRIN AL MULHIM[1], HUSAM ALMUHAISH[2], SHAHID BASHIR[1,3] and TALAL M. AL-HARBI[1]

[1]Department of Neurology, Neuroscience Center, King Fahad Specialist Hospital-Dammam, Dammam 32253-3202, Kingdom of Saudi Arabia; [2]Neuroradiology Section, Medical Imaging Service Center, King Fahad Specialist Hospital-Dammam, Dammam 32253-3202, Kingdom of Saudi Arabia; [3]King Salman Center for Disability Research, Riyadh 11614, Kingdom of Saudi Arabia

Received November 12, 2024; Accepted March 12, 2025

DOI: 10.3892/br.2025.1976

Abstract. Hyperammonemic encephalopathy is a life-threatening condition that can lead to coma and death due to brain edema and intracranial hypertension. The current study presents the clinical and magnetic resonance imaging (MRI) findings of 5 cases of acute hyperammonemic hepatic encephalopathy. MRI images of all 5 patients showed diffuse cortical swelling affecting the frontal, temporal, and parietal lobes, as well as the insular cortex and cingulate gyri. However, the underlying white matter, peri-rolandic area, and posterior occipital lobe remained unaffected. These specific brain MRI features are more commonly observed in cases with 165 μmol/l or higher ammonia levels, suggesting a potential correlation. Further studies are needed to confirm this association.

Introduction

Hyperammonemia is a potential complication of chronic or acute liver disease, as well as various non-hepatic conditions. The causes of hyperammonemia in adults can generally be divided into two main categories: Increased ammonia production (such as via infection, high protein load, multiple myeloma, and renal failure) and decreased ammonia elimination (such as from liver failure, drugs, and inborn errors of metabolism) (1). However, hyperammonemia is often caused by severe liver disease. In fact, the incidence of hyperammonemia in hepatic encephalopathy (HE) is as high as 90% (2). Clinically, HE is a group of neuropsychiatric signs and symptoms in patients with liver disease or a portosystemic shunt. HE can be reversed by early treatment of the underlying causes (3,4). Neuroimaging, particularly magnetic resonance imaging (MRI), plays a vital role in elucidating the neural mechanisms underlying HE (5). The brain MRI of patients with chronic HE typically shows cerebral atrophy and bilateral symmetrical hyperintensities of the globus pallidus on T1-weighted images without corresponding signal intensity in T2-weighted images (6,7). Conversely, acute hyperammonemic encephalopathy often presents bilateral symmetrical cortical signal abnormalities with corresponding signal intensity changes in T2-weighted images and diffusion restriction (7-10).

The current study aims to present the clinical characteristics and brain MRI findings of acute HE associated with hyperammonemia in 5 adult patients.

Case report

Patients and methods. This retrospective case series study included 5 patients >18 years of age, treated between January 2016 and December 2021 at King Fahad Specialist Hospital-Dammam (KFSH-D) (Dammam, Saudi Arabia). The patients were all identified to have documented hyperammonemic HE. The study was approved by the Ethics Committee of King Fahad Specialist Hospital Dammam (IRB-Pub-024-01). Written informed consent for publication was obtained from all subjects. Clinical and laboratory data were collected using electronic medical records for each patient. All 5 patients were critically ill in the intensive care unit (ICU) due to a decline in their level of consciousness. The patients underwent an MRI of the brain 3-10 days after the onset of symptoms. A neuroradiologist analyzed all the images. The common clinical features of the patients were that they presented with decreased levels of consciousness secondary to acute hepatic failure with hyperammonemia. The brain MRI of each patient was performed using a 3-T MRI scanner (Magnetom Skyra; Siemens Healthineers) with a 20-channel phased array head coil. The imaging protocol included axial and sagittal T1-weighted images, axial and coronal T2-weighted images, axial fluid-attenuated inversion recovery (FLAIR), axial susceptibility weighted imaging, axial echo-planar

Correspondence to: Dr Talal M. Al-Harbi, Department of Neurology, Neuroscience Center, King Fahad Specialist Hospital-Dammam, 6830 Ammar Bin Thabet Street, Al Merikbat, Dammam 32253-3202, Kingdom of Saudi Arabia
E-mail: talal563@yahoo.com

Key words: acute hyperammonemic encephalopathy, magnetic resonance imaging, diffusion-weighted imaging, hepatic encephalopathy, hyperammonemia

diffusion-weighted imaging and apparent diffusion coefficient map. Additional axial and sagittal T1-weighted images were recorded for 2 patients after administering the intravenous contrast agent.

Results. A total of 5 patients (2 men and 3 women) were included in this study (Table I). The causes of hepatic failure were metastatic colon cancer, chronic inflammatory hepatitis in the background of sickle cell anemia, primary sclerosing cholangitis associated with ulcerative colitis, autoimmune hepatitis, and post-bypass surgery steatohepatitis, respectively. Plasma ammonia levels ranged from 165 to 512 μmol/l (normal range, 11-32 μmol/l). Diffuse cortical swelling was observed in the MRI brain scans of all patients, involving the frontal, temporal, and parietal lobes, as well as the insula. The underlying white matter, peri-rolandic area, and posterior occipital lobe were spared. These cortical MRI abnormalities have been shown to worsen with increased ammonia levels (Table I). In 4 of the 5 patients, the bilateral thalami were affected, and another patient showed a few focal ischemic lesions in the caudothalamic groove and splenium of the corpus callosum. Of the 5 patients, 2 survived, while 3 died due to septic shock and multiorgan failure.

Case 1. A 37-year-old man with a known case of colon adenocarcinoma with liver metastasis was admitted electively in November 2017 under the care of the hepatobiliary team at KFSH-D for a hepatectomy. However, the procedure was complicated by portal vein air thrombosis and hypotension, necessitating an ICU admission. The serum ammonia level was significantly elevated at 165 μmol/l. Additionally, liver enzymes were increased, with an aspartate transferase (AST) level of 105 U/l (normal range, 8-38 U/l), an alanine aminotransferase (ALT) level of 228 U/l (normal range, 17-45 U/l), a total bilirubin level of 211 μmol/l (normal range, 4-21 μmol/l) and an international normalized ratio (INR) of 2.4 (normal range, 0.80-1.20). The patient's level of consciousness remained low even after sedation was stopped. Initially, the patient [Glasgow Coma Scale (GCS) score of 6/15] could open their eyes in response to painful stimulation, but had no verbal or motor responses, although the brainstem reflexes were intact.

Routine electroencephalography (EEG) showed generalized slowing within the delta range and no epileptiform discharges or electrographic seizures. The brain MRI on the seventh day post-surgery demonstrated bilateral symmetrical cortical edema with marked diffusion restriction involving the insula, temporal lobe, cingulate gyrus, and thalami (Fig. 1). After 10 days, the patient's condition deteriorated even more. The liver enzymes increased (AST, 84 U/l; ALT, 139 U/l; and total bilirubin, 245 μmol/l), and the serum ammonia level reached 188 μml/l due to acute liver failure. A subsequent follow-up MRI revealed an increase in bilateral symmetrical, predominantly cortical edema, with intermediate signal intensity on T2/FLAIR, but a decrease in diffusion restriction (Fig. 2). The patient exhibited marked improvement gradually throughout the month following the liver transplant. A follow-up was conducted in the clinic 2 months after discharge, and the patient was doing well. Furthermore, the follow-up lab results indicated a significant recovery of liver enzymes, with AST at 23 U/l, ALT at 24 U/l, and serum ammonia at 19 μml/l. However, the patient declined further brain imaging due to the resolution of the symptoms.

Case 2. A 27-year-old man with a known history of sickle cell disease and chronic inflammatory hepatitis was admitted to the ICU of the Procare Hospital (Khobar, Saudi Arabia) with low consciousness and severe jaundice. In December 2018, the patient was transferred to KFSH-D, where a diagnosis of decompensated liver failure complicated by disseminated intravascular coagulation and multiorgan failure was formed based on clinical and laboratory findings. During the physical examination, it was observed that the patient was in a deep coma, with a GCS score of 3 out of 15 and intact brainstem reflexes. The patient exhibited generalized hypotonia and did not respond to painful stimuli. The deep tendon reflexes were decreased, and there was no bilateral reaction in the plantar reflexes.

Laboratory tests showed leukocytosis, with a white blood cell count of 28.3×10^9/l (normal range, $3.4\text{-}9.6 \times 10^9$/l), a low hemoglobin level of 5.8 g/dl (normal range, 13.6-16.9 g/dl), thrombocytopenia, with a platelet count of 58×10^3/l (normal range, $152\text{-}324 \times 10^3$/l), and a high ammonia level of 193 μmol/l. Liver function tests indicated a total bilirubin level of 886 μmol/l, a conjugated bilirubin level of 809 μmol/l (normal range, 0.8-3.0 μmol/l), an alkaline phosphatase (ALP) level of 405 U/l (normal range, 54-144 U/l), an ALT level of 137 U/l (normal range, 17-45 U/l) and an AST level of 263 U/l (normal range, 8-38 U/l). Renal function was also elevated, with a blood urea nitrogen (BUN) level of 50 mmol/l (normal range, 2.1-8.5 mmol/l) and a creatinine level of 256 μmol/l (normal range, 61.9-114.9 μmol/l). The brain MRI, taken 8 days post-admission (Fig. S1), showed bilateral, nearly symmetric cortical swelling, with FLAIR/T2 high signal intensity and diffusion restriction affecting the frontal, parietal, and temporal regions while sparing the peri-rolandic and occipital areas. The patient's clinical condition deteriorated steadily, and they succumbed to septic shock and multiorgan failure 2 weeks later.

Case 3. A 36-year-old woman with ulcerative colitis (UC) underwent a deceased donor liver transplant (split liver) smooth surgery hepaticojejunostomy for primary sclerosing cholangitis in Feb 2021 at KFSH-D, and recovered without any complications. However, on the fifth day after surgery the patient's level of consciousness began to deteriorate. During a physical examination, while not sedated, it was noted that the patient had an elevated temperature of 38.1°C, generalized jaundice, and a GCS score of 4 out of 15. The patient later experienced multiple generalized tonic-clonic convulsions, and the EEG showed generalized background slowing with epileptiform discharges. At that time, laboratory tests revealed high level of ammonia (512.75 μmol/l), liver enzymes (total bilirubin, 344.6 μmol/l; conjugated bilirubin, 259 μmol/l; ALP, 118 U/l; ALT, 1,325 U/l; and AST, 1,856 U/l) and renal function (BUN, 10.5 mmol/l; and creatinine, 179 μmol/l). The seizures were controlled using a midazolam infusion at 2 mg/h for 3 days. An MRI of the brain 3 days later showed diffuse symmetrical cerebral edema with high signal intensity and diffusion restriction, sparing the bilateral occipital lobes and

Table I. Clinical summary of cases reported.

Characteristic	Case 1	Case 2	Case 3	Case 4	Case 5
Age, years	37	27	36	18	51
Sex	Male	Male	Female	Female	Female
Diagnosis	Acute liver failure secondary to liver surgery	Decompensated liver failure	Acute graft rejection post-liver transplant	Acute liver failure secondary to autoimmune hepatitis	Acute-on-chronic steatohepatitis
GCS	4/15	3/15	4/15	4/15	5/15
Presence of seizures	No	No	Yes	Yes	Yes
Liver enzymes, U/l[a]	AST, 105; ALT, 228	AST, 263; ALT, 137	AST, 1,856; ALT, 1,325	AST, 1,914; ALT, 5,075	AST, 93; ALT, 63
Ammonia level, μmol/l[b]	165-188	193	512.75	310	174
Total bilirubin μmol/l[c]	211	886	344.6	334	158
Period between onset of symptoms and MRI, days	7	8	3	5	10
Area of brain involvement in MRI	Insular cortex, frontal lobe sparing the peri-rolandic region, posterior temporal lobe, anterior cingulate gyrus and the bilateral anterolateral thalami	Insular cortex, frontal lobe sparing the peri-rolandic region, temporal lobe, parietal lobe, and anterior cingulate gyri	Insular cortex, frontal lobe sparing the peri-rolandic region, temporal lobe, parietal lobe, anterior and posterior cingulate gyri, and the bilateral thalami	Insular cortex, frontal lobe sparing the peri-rolandic region, temporal lobe, parietal lobe, anterior and posterior cingulate gyri, and the bilateral posteromedial thalami	Insular cortex, frontal lobe sparing the peri-rolandic region, posterior temporal lobe, parietal lobe, and anterior cingulate gyrus.
Outcome	Recovered	Died	Died	Died	Recovered

[a]AST normal range, 8-38 U/l; and ALT normal range, 17-45 U/l. [b]Ammonia normal range, 11-32 μmol/l. [c]Total bilirubin normal range, 4-21 μmol/l. GCS, Glasgow Coma Scale; MRI, magnetic resonance imaging; AST, aspartate transferase; ALT, alanine aminotransferase.

peri-rolandic region (Fig. S2). The patient passed away on the next day.

Case 4. An 18-year-old woman with autoimmune hepatitis was transferred from Aramco Hospital (Dhahran, Saudi Arabia) to the ICU at KFSH-D in February 2020. The patient had acute liver failure, decreased consciousness, and a new left-sided focal unaware seizure. The seizure was aborted after receiving levetiracetam loading of 3,000 mg over 10 min and a midazolam infusion of 2 mg/h over 24 h. The initial computed tomography brain scan (CT) showed cerebral edema, diffuse sulcal effacement, and crowding of the foramen magnum. The patient underwent a liver transplant procedure. Brain MRI 3 days later showed diffuse symmetrical cerebral cortical abnormalities with high signal intensity on T2-weighted imaging and FLAIR, affecting the splenium of the corpus callosum, the left Globus pallidus, bilateral thalamic regions, the posterior limb of the internal capsule, and the hippocampi. This was associated with diffusion restriction, but the occipital lobes and peri-rolandic region were spared (Fig. S3). After withdrawing the midazolam infusion, the physical examination showed a GCS score of 4 out of 15, with all brainstem reflexes intact, generalized hypotonia and hyperreflexia, and unresponsive plantar reflexes. Laboratory tests revealed an ammonia level of 310 μmol/l and elevated liver enzymes, with an ALT level of 5,075 U/l, an AST level of 1,914 U/l, and a total bilirubin level of 334 μmol/l.

A follow-up EEG showed a generalized slowing in the delta range, and no epileptiform discharges were present. Additionally, a follow-up MRI, conducted 10 days after the initial scan, showed interval evolution of the intraparenchymal changes (Fig. S4). The patient passed away due to septic shock and multiorgan failure after 39 days in the ICU.

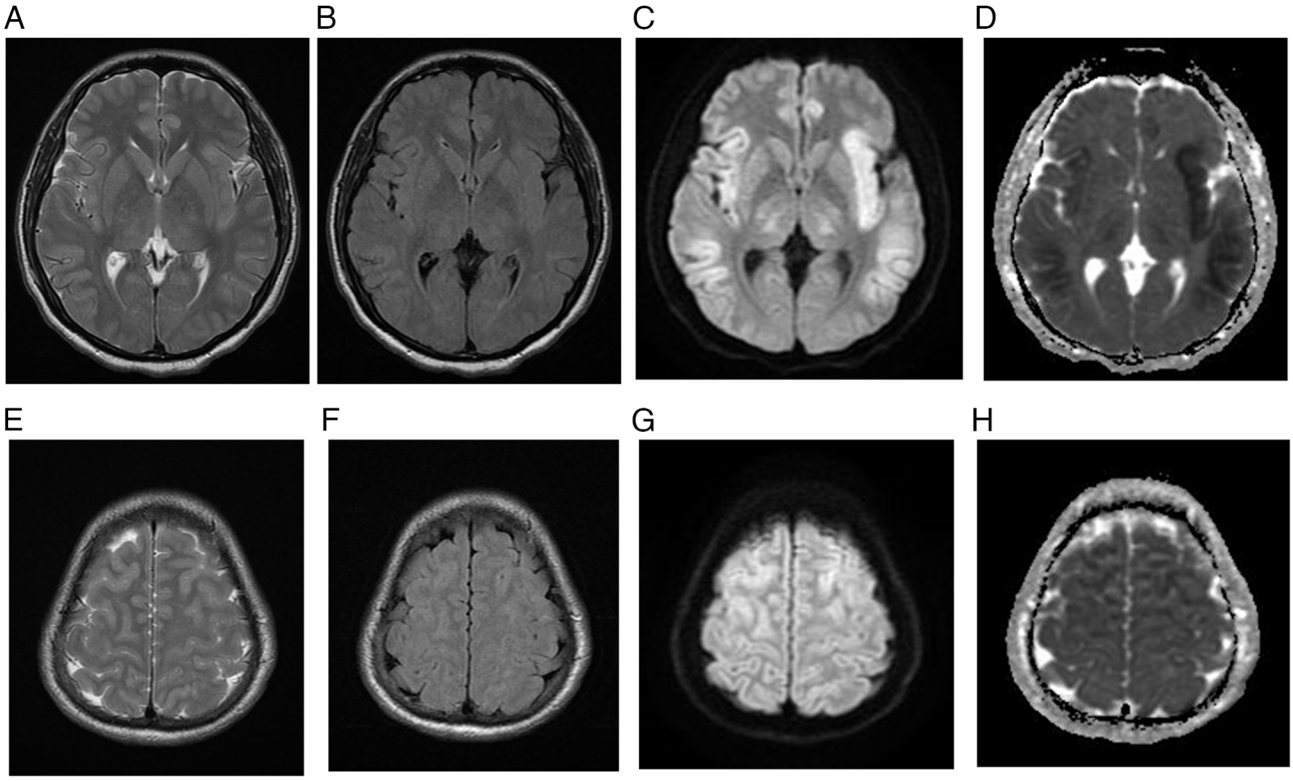

Figure 1. Initial brain MRI for case 1. (A) T2-weighted MRI, (B) FLAIR, (C) DWI and (D) ADC map demonstrating asymmetric cortical high T2 and FLAIR signal intensity involving the bilateral insular cortex, temporal lobes, cingulate gyri and bilateral lateral thalami with corresponding diffusion restriction. The bilateral occipital lobes are spared. At the level of vertex, (E) T2-weighted image, (F) FLAIR image, (G) DWI and (H) ADC map demonstrating symmetric cortical high T2 and FLAIR signal intensities involving the frontal and parietal lobes with corresponding restricted diffusion. The bilateral peri-Rolandic regions are spared. FLAIR, fluid-attenuated inversion recovery; DWI, diffusion-weighted imaging; ADC, apparent diffusion coefficient.

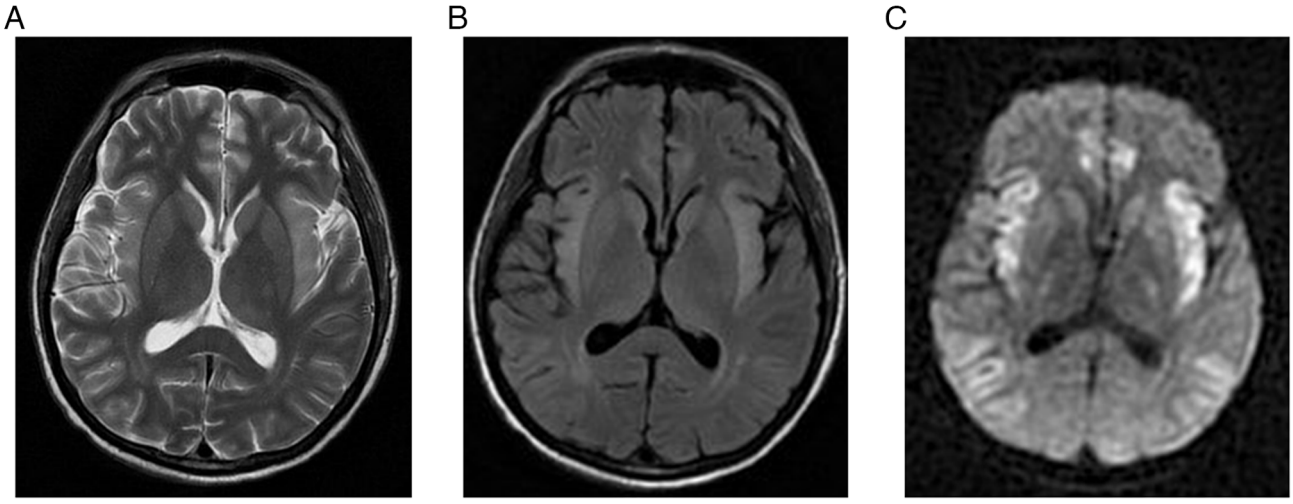

Figure 2. Follow-up MRI brain scan for case 1 after 2 weeks. (A) T2-weighted MRI, (B) fluid attenuated inversion recovery image and (C) diffusion-weighted imaging demonstrating slight interval progression of symmetric cortical high T2 and FLAIR signal intensities involving the bilateral insular cortex, temporal lobes, cingulate gyri and bilateral thalami. Mild regression of diffusion restriction suggests evolutionary changes. Interval generalized atrophic brain changes are noted, evidenced by a prominent ventricular system and cerebral sulci. MRI, magnetic resonance imaging.

Case 5. A 51-year-old woman with a known case of hypothyroidism and a history of gastric bypass surgery complicated by steatohepatitis presented with impaired consciousness and jaundice. The patient was admitted to KFSH-D in December 2018 through the Emergency Department with acute-on-chronic liver failure and pulmonary edema that required intubation. The patient's level of consciousness deteriorated within 3 days. Upon examination, the patient was unresponsive, with a GCS of 5 out of 15, and preserved brainstem reflexes. Laboratory investigations revealed a high serum ammonia level of 174 μmol/l, mildly elevated liver enzymes (AST, 93 U/l; and ALT, 63 U/l), and a total bilirubin level

of 158 μmol/l. The EEG results showed generalized slowing of the background without epileptiform discharges. A brain MRI scan performed 10 days after the onset of symptoms showed bilateral asymmetric cortical swelling and diffusion restriction in the insula, cingulate gyri, and bilateral hippocampi, with corresponding T2/FLAIR hyperintensity and T1 hyperintensity sparing the occipital lobes and peri-rolandic region (Fig. S5). The patient experienced a prolonged generalized convulsion for 30 min, which was controlled with levetiracetam in a 3,000-mg intravenous infusion over 15 min, followed by 750 mg orally twice and lamotrigine at 50 mg twice. The patient's condition improved as the seizure subsided and the ammonia level normalized, but residual memory impairment was still present. A follow-up brain MRI revealed complete resolution of the cortical and subcortical T2 and FLAIR high signal intensities, along with marked bilateral symmetrical brain atrophy (Fig. S6). The patient was regularly followed up by the neurology team and remained seizure-free after adding phenytoin at 100 mg every 12 h to the treatment, but still complains of memory impairment.

Discussion

Despite the diverse and complex presentations of the 5 patients in the present study, the clinical courses were characterized by the interplay of acute hepatic failure superimposed on preexisting chronic liver disease. This resulted in a rapid rise in serum ammonia levels, leading to a marked decline in consciousness and the development of HE. Simultaneously, brain MRI revealed extensive cortical signal-intensity changes with associated restricted diffusion. Regardless of the primary etiology, the patients eventually shared similar MRI brain findings that showed bilateral symmetrical involvement of the insular cortex and cingulate gyri on FLAIR and T2-weighted imaging sequences, with diffusion restriction sparing the peri-rolandic and occipital areas. These widespread cortical lesions may represent hyperammonemia-related brain edema (3,8) and have been reported previously in several case series (8-12). For example, U-King-Im *et al* (8) reported the cases of 4 patients with similar findings, 3 of whom had liver damage due to acute hepatic failure and sepsis with a background of chronic liver diseases (8). The extensive cortical brain MRI abnormalities seen in these patients could be indicative of other conditions, such as hypoxic-ischemic encephalopathy, limbic encephalitis, acute hypertension, hyponatremia, or Creutzfeldt-Jakob disease (13). However, none of the patients in the present study exhibited clinical or laboratory evidence supporting these conditions.

Notably, the peri-rolandic and occipital areas are usually relatively spared in hyerammonemic encephalopathy (10). A recent report detailed the cases of 3 patients with hyperammonemic encephalopathy stemming from different causes, including infectious, toxic, and cirrhotic origins, all of which demonstrated similar findings on MRI (9). Furthermore, Takanashi *et al* (14) described 3 cases of hyperammonemia encephalopathy secondary to late-onset ornithine transcarbamylase deficiency, each showing evidence of injury to the cingulate and insular cortices (14). This later study also indicated that the peri-rolandic and occipital cortices were spared. The authors proposed the vulnerability of the cingulate gyrus and insular cortex due to hyperammonemia-hyper glutaminergic encephalopathy (14). This unique sparing pattern is significant, as it can help differentiate hyperammonemic encephalopathy from other conditions with similar MRI findings. However, it remains unclear why certain brain areas, such as the insular cortex or cingulate gyrus, appear especially susceptible to the toxic effects of ammonia.

The involvement of various brain structures, including the thalami, basal ganglia, periventricular white matter, brainstem, and peri-rolandic and occipital cortical regions, has been inconsistently reported in patients with hyperammonemic encephalopathy (8,15,16). In the present cases, in addition to the insular and cingulate gyri, the thalami were affected in the MRI of patients 1, 3, 4, and 5, possibly due to their chronic liver diseases. However, a premorbid brain MRI was not available to rule out this possibility.

In the ICU, the patients experienced a range of systemic complications, including acute renal failure, seizure, and sepsis. These issues may have contributed to the MRI changes observed. However, not every patient faced these complications, yet they all displayed similar MRI cortical signal abnormalities. The symmetrical changes in the insular and cingulate gyri suggest a toxic effect. Additionally, the resemblance of the MRI findings in the present cases to those reported in the previous literature (5,8,9,10,12,14), even in patients without hepatic failure, seizure or hypoxic-ischemic injury, strongly supports the idea that the brain MRI changes described are directly linked to hyperammonemia.

Ammonia is produced through protein metabolism in the gastrointestinal tract, with the liver being the primary site of ammonia breakdown in the urea cycle. Elevated serum ammonia levels indicate compromised hepatic function or the presence of a portosystemic shunt. Ammonia can cross the blood-brain barrier through diffusion in its unionized form (NH_3) and active transport in its ionized form (NH_4^+) (17). Astrocytes utilize ammonia to generate high concentrations of glutamine (17), rapidly increasing cellular osmolarity as glutamine accumulates, leading to astrocyte swelling and heightened intracranial pressure (18). Furthermore, hyperammonemia disrupts brain energy metabolism, causing an increase in the lactate-to-pyruvate ratio (17). Conversely, brain edema is less common in cases of chronic liver failure, as there is sufficient time for compensatory cellular adaptation mechanisms to respond to osmotic changes (19).

All patients in the present case series had high serum levels of ammonia. However, in cases 1 and 4, an association was observed between serum ammonia levels, deterioration of consciousness, and cortical MRI changes. Higher ammonia levels appeared to lead to deeper comas and increased cortical brain MRI hyperintensities. This association has also been noted in previous reports (8,20). By contrast, plasma ammonia levels are often measured in clinical settings to assist in the diagnosis; these results should be interpreted cautiously, as elevated ammonia levels can arise from various conditions apart from acute liver failure, such as the administration of drugs (e.g., sodium valproate and chemotherapy), infections, hypothyroidism, multiple

myeloma, inborn errors of metabolism, and post-lung or -bone marrow transplantation (11,12,20-23).

Prolonged and high serum hyperammonemia levels can lead to significant brain injuries and devastating complications, such as brain edema and herniation. In the long term, insular and cingulate atrophy may occur (12,21,23-25). Therefore, timely recognition and treatment of hyperammonemia are crucial to avoid these complications. In the present study, patients 2, 3, and 4 exhibited elevated serum ammonia levels and sustained more extensive brain injuries, resulting in poor prognoses. Conversely, patients 1 and 5, who had lower serum ammonia levels, survived after their plasma ammonia levels normalized, although patient 5 experienced residual memory impairment, likely due to prolonged seizure activity and hyperammonemia encephalopathy. The main limitations of the present study are its retrospective design and the lack of baseline imaging and laboratory data before the recent admission, which warrants the need for future studies with larger cohorts and prospective designs to perform correlational analyses between blood ammonia levels and cerebral injury, and to strengthen the understanding of this association in similar populations.

In conclusion, the current study presented the cases of 5 adult patients who exhibited typical brain MRI features of acute hyperammonemic HE. These patients demonstrated symmetrical signal abnormalities in the insular and cingulate cortices, while the peri-rolandic and occipital cortices were spared. Early recognition of these diagnostic features could lead to improved patient outcomes through proper treatment intervention. Furthermore, an association was noted between serum ammonia levels and brain MRI abnormalities, which warrants further investigation in future studies.

Acknowledgements

Not applicable.

Funding

The King Salman center For Disability Research funded this work through Research Group no. KSRG-2024-307.

Availability of data and materials

The data generated in the present study may be requested from the corresponding author.

Authors' contributions

AB was responsible for the design of the study and overall project coordination. HA, SO, NA, FA and SM contributed to data collection and assisted with the literature review and manuscript drafting. HA and HA provided radiological and clinical oversight and supported the validation of results. SB structured and critically revised the manuscript and secured funding. TAH contributed to the conceptual framework and provided overall project supervision. AB and TAH confirm the authenticity of all the raw data. All authors have read and approved the final manuscript.

Ethics approval and consent to participate

The study was approved by the Ethics Committee of King Fahad Specialist Hospital-Dammam (IRB-Pub-024-01).

Patient consent for publication

Written informed consent for publication was obtained from all subjects.

Competing interests

The authors declare that they have no competing interests.

References

1. Hussain J, Schlachterman A, Kamel A and Gupte A: Hyperinsulinism hyperammonemia syndrome, a rare clinical constellation. J Investig Med High Impact Case Rep 4: 2324709616632552, 2016.
2. Brusilow SW: Hyperammonemic encephalopathy. Medicine (Baltimore) 81: 240-249, 2002.
3. Atluri DK, Prakash R and Mullen KD: Pathogenesis, diagnosis, and treatment of hepatic encephalopathy. J Clin Exp Hepatol 1: 77-86, 2011.
4. Dharel N and Bajaj JS: Definition and nomenclature of hepatic encephalopathy. J Clin Exp Hepatol 5 (Suppl 1): S37-S41, 2015.
5. Zhang XD and Zhang LJ: Multimodal MR imaging in hepatic encephalopathy: State of the art. Metab Brain Dis 33: 661-671, 2018.
6. Morgan MY: Cerebral magnetic resonance imaging in patients with chronic liver disease. Metab Brain Dis 13: 273-290, 1998.
7. Rosario M, McMahon K and Finelli PF: Diffusion-weighted imaging in acute hyperammonemic encephalopathy. Neurohospitalist 3: 125-130, 2013.
8. U-King-Im JM, Yu E, Bartlett E, Soobrah R and Kucharczyk W: Acute hyperammonemic encephalopathy in adults: Imaging findings. AJNR Am J Neuroradiol 32: 413-418, 2011.
9. Reis E, Coolen T and Lolli V: MRI findings in acute hyperammonemic encephalopathy: Three cases of different etiologies: Teaching point: To recognize MRI findings in acute hyperammonemic encephalopathy. J Belg Soc Radiol 104: 9, 2020.
10. Arnold SM, Els T, Spreer J and Schumacher M: Acute hepatic encephalopathy with diffuse cortical lesions. Neuroradiology 43: 551-554, 2001.
11. Lora-Tamayo J, Palom X, Sarrá J, Gasch O, Isern V, Fernández de Sevilla A and Pujol R: Multiple myeloma and hyperammonemic encephalopathy: Review of 27 cases. Clin Lymphoma Myeloma 8: 363-369, 2008.
12. Bindu PS, Sinha S, Taly AB, Christopher R and Kovoor JME: Cranial MRI in acute hyperammonemic encephalopathy. Pediatr Neurol 41: 139-142, 2009.
13. Koksel Y, Benson J, Huang H, Gencturk M and McKinney AM: Review of diffuse cortical injury on diffusion-weighted imaging in acutely encephalopathic patients with an acronym: 'CRUMPLED'. Eur J Radiol Open 5: 194-201, 2018.
14. Takanashi J, Barkovich AJ, Cheng SF, Weisiger K, Zlatunich CO, Mudge C, Rosenthal P, Tuchman M and Packman S: Brain MR imaging in neonatal hyperammonemic encephalopathy resulting from proximal urea cycle disorders. AJNR Am J Neuroradiol 24: 1184-1187, 2003.
15. McKinney AM, Lohman BD, Sarikaya B, Uhlmann E, Spanbauer J, Singewald T and Brace JR: Acute hepatic encephalopathy: Diffusion-weighted and fluid-attenuated inversion recovery findings, and correlation with plasma ammonia level and clinical outcome. AJNR Am J Neuroradiol 31: 1471-1479, 2010.
16. McPhail MJW, Patel NR and Taylor-Robinson SD: Brain imaging and hepatic encephalopathy. Clin Liver Dis 16: 57-72, 2012.
17. Ott P and Vilstrup H: Cerebral effects of ammonia in liver disease: Current hypotheses. Metab Brain Dis 29: 901-911, 2014.
18. Hertz L and Kala G: Energy metabolism in brain cells: Effects of elevated ammonia concentrations. Metab Brain Dis 22: 199-218, 2007.

19. Rovira A, Alonso J and Córdoba J: MR imaging findings in hepatic encephalopathy. AJNR Am J Neuroradiol 29: 1612-1621, 2008.
20. Wang V and Saab S: Ammonia levels and the severity of hepatic encephalopathy. Am J Med 114: 237-238, 2003.
21. Clay AS and Hainline BE: Hyperammonemia in the ICU. Chest 132: 1368-1378, 2007.
22. Lichtenstein GR, Yang YX, Nunes FA, Lewis JD, Tuchman M, Tino G, Kaiser LR, Palevsky HI, Kotloff RM, Furth EE, *et al*: Fatal hyperammonemia after orthotopic lung transplantation. Ann Intern Med 132: 283-287, 2000.
23. Chou HF, Yang RC, Chen CY and Jong YJ: Valproate-induced hyperammonemic encephalopathy. Pediatr Neonatol 49: 201-204, 2008.
24. Nott L, Price TJ, Pittman K, Patterson K and Fletcher J: Hyperammonemia encephalopathy: An important cause of neurological deterioration following chemotherapy. Leuk Lymphoma 48: 1702-1711, 2007.
25. Liu J, Lkhagva E, Chung HJ, Kim HJ and Hong ST: The pharmabiotic approach to treat hyperammonemia. Nutrients 10: 140, 2018.